109

COMBUSTION OF LIQUID MONOPROPELLANTS AND BIPROPELLANTS IN DROPLETS

By C. SANCHEZ TARIFA, P. PEREZ DEL NOTARIO AND F. GARCIA MORENO

Introduction

Theoretical and experimental results of an investigation on the combustion or decomposition of monopropellant droplets in an inert atmosphere, and on the combustion of bipropellant systems consisting of fuel (oxidizer) droplets in the vapor of an oxidizer (fuel) are given in the present work.

Combustion of droplets has been mainly investigated for the case of fuel drops burning in air. Theoretical studies[1, 2, 4, 7, 9, 10, 11] have been carried out by assuming that the reaction rate is infinitely rapid. Such an assumption implies that chemical reaction occurs at a zero-thickness layer, where the mass fractions of both fuel and ozidizer become equal to zero. On the basis of this assumption, which disregards chemical kinetics, it was found that the burning rate is proportional to the droplet radius, and, therefore, that the square of the droplet radius is a linear function of time. It was also found that the flame:droplet radius ratio does not depend upon the droplet radius.

For droplets larger than 100 to 200 μ in diam and at pressures equal or higher than one atmos, the above-mentioned linear law has been experimentally verified on several occasions,[1–4, 7, 9, 10, 11] and the theoretical and experimental values of the burning rate were in good agreement.

On the contrary, experimental values of the flame:droplet radius ratio did not coincide with the theoretical ones and, what is more significant, the observed values of these ratios were not constant, but they increased as the droplet radius decreased.[4, 10]

Such lack of agreement was at first attributed to the influence of natural convection, but Kumagai and Isoda[10, 11] found similar results in a zero-gravity field. These investigators explained the difference between theoretical and experimental results by means of an approximated theory on the transient combustion of droplets. However, transient conditions alone cannot explain such effects, because Wise, Lorell and Wood[4] obtained, for steady-state combustion, similar laws of variation of the flame-droplet radius ratio as a function of the droplet radius by using the porous sphere technique.

There are no experimental results on the combustion of droplets at low pressure and very little experimental evidence on the combustion of small droplets. Hall and Diederichsen[3] and Bolt[9] found values of the evaporation constant for droplets of about 200 μ, smaller in diameter than those obtained for large droplets, but these differences were attributed to the experimental techniques.

Lorell, Wise and Carr[5] studied the combustion of droplets considering finite chemical kinetics, and solved the problem by integrating numerically the differential equations of the process. However, they considered a fixed value of the droplet radius, which was rather large, and they studied the problem taking equal values of both molecular weights and Lewis-Semenov numbers. For these conditions, results obtained by assuming an infinite reaction rate are not very different from those derived considering finite chemical kinetics.

In the present work combustion of droplets will be studied considering chemical kinetics, diffusion of species of different molecular weight and different Lewis-Semenov numbers. It will be shown that for an infinite reaction rate an asymptotic solution of the problem is obtained,

which is only strictly applicable when either the droplet radius or the pressure tends to an infinite value.

In general, results tend rapidly toward their asymptotic values. However, for small droplets or at low pressure, important errors may be introduced by assuming that the reaction rate is infinitely fast. For example, theoretical results show that, under certain values of either the pressure or the droplet radius, combustion seems impossible. This important theoretical conclusion, which does not appear when chemical kinetics is disregarded, has been experimentally verified. The errors introduced by disregarding chemical kinetics may be especially important when the molecular weight of the gaseous reactant is much smaller than the molecular weight of the liquid reactant, as for the case of the combustion of oxygen droplets in a hydrogen atmosphere.

Combustion of monopropellant droplets has been the subject of several works.[6, 8, 12, 13, 14] In this process the flame is of the premixed type. Therefore, the assumption of taking an infinite reaction rate, which may give approximate results for diffusion flames, is not applicable.

In the present work it will be shown that chemical kinetics influences decisively the process and that the controlling parameter is the ratio of the activation energy to the heat of reaction. Experimental evidence on the combustion of monopropellant droplets is almost absent. Therefore, an accurate comparison between experimental and theoretical results cannot be realized.

Fundamental Assumptions

Combustion of both monopropellant and bipropellant droplets will be studied under the following assumptions. The droplets are considered to be isolated and at rest, and the process is assumed to have spherical symmetry. Therefore, the influence of natural convection is disregarded. The process is stationary. Under such conditions the study is only strictly applicable to the combustion of constant radius droplets fed with a fuel flow equal to the amount of fuel which is evaporated and burned.

However, it has been shown that for large or medium sized droplets the errors introduced by considering steady-state conditions are not important. This is due to the fact that radial velocity of the droplet surface is small as compared to the diffusion velocities of the species. For this reason, results obtained by using porous spheres of constant diameters are similar to those obtained by burning real liquid droplets.

Nevertheless, theoretical results obtained for small droplets will show that the influence of the droplet radius on the process may be very important in certain cases. For these special conditions the steady-state assumption no longer holds.

In order to obtain general conclusions, only reactant species and reaction products will be considered, and the actual chemical kinetics of the process will be approximated by means of over-all reactions of n^{th} order. However, the analytical method used to solve the problem is applicable to more complicated kinetic schemes.[8, 13]

For simplicity, average values will be adopted for the thermal conductivity and for the specific heat of the mixture. The gas pressure will be considered constant throughout the process and the heat transferred to the droplet surface through radiation will be neglected.

General Equations

Under the aforementioned assumptions, the general equations of the process are as follows:

CONTINUITY

For each species, we have:

$$\frac{m}{4\pi r^2}\frac{d\epsilon_i}{dr} = w_i \,. \tag{1}$$

If ν_i represents the stoichiometric coefficients of the over-all reaction, molecular weights, M_i, and the reaction rates, w_i, are related as follows,

$$\frac{w_i}{\nu_i M_i} = \pm\frac{w_j}{\nu_j M_j} \,, \tag{2}$$

we have:

$$\frac{\epsilon_i - \epsilon_{is}}{\nu_i M_i} = \pm\frac{\epsilon_j - \epsilon_{js}}{\nu_j M_j} \,. \tag{3}$$

ENERGY

The equation of energy is given by:

$$m\Big(\sum_i h_i \epsilon_i - \sum_i h_{is}\epsilon_{is} + q_l\Big) - 4\pi r^2 \bar{\lambda}\frac{dT}{dr} = 0. \tag{4}$$

Expressing the enthalpies as a function of the temperature, we have:

$$m[\sum_i(\epsilon_i - \epsilon_{is})h_i^0 + (T - T_0)\sum_i c_{pi}\,\epsilon_i - (T_s - T_0)\sum_i c_{pi}\,\epsilon_{is} + q_l] - 4\pi r^2\bar{\lambda}\frac{dT}{dr} = 0. \quad (5)$$

Introducing the heat of reaction by means of relations (3), taking an average value for the specific heats, and referring the equation to the combustion products of Equation (3), we obtain:

$$m[\bar{c}_p(T - T_s) - q_r\,\epsilon_3 + q_l] - 4\pi r^2\bar{\lambda}\frac{dT}{dr} = 0. \quad (6)$$

DIFFUSION

Assuming that only concentration diffusion exists, we have:

$$\sum_j \frac{Y_j}{M_j}\left[\frac{m\bar{c}_p}{4\pi r^2\bar{\lambda}}\left(\frac{\epsilon_j}{Y_j} - \frac{\epsilon_i}{Y_i}\right)\mathfrak{L}_{ij} - \frac{1}{Y_i}\frac{dY_i}{dr} + \frac{1}{Y_j}\frac{dY_j}{dr}\right] = 0. \quad (7)$$

BOUNDARY CONDITIONS

It will be assumed that liquid phase reactions do not exist and that there is only one liquid chemical species.[a] It will also be assumed that the chemical reaction goes to completion at infinity and that the temperature and composition of the atmosphere at infinity are known. Thus, we have:

$$r = r_s\begin{cases} T = T_s \\ \epsilon_{1s} = 1 \\ \epsilon_{is} = 0 \quad (i \neq 1) \end{cases} \qquad r = \infty\begin{cases} T = T_\infty \\ Y_{1\infty} = 0 \rightarrow \epsilon_{1\infty} = 0. \\ Y_i = Y_{i\infty} \end{cases} \quad (8)$$

There exists one boundary condition in excess of the number of differential equations, which gives the burning rate m, or "eigenvalue" of the system.

[a] No distinction will be made between the species of a monopropellant composed of a mixture of fuel and oxidizer.

Solution of the System

Solution of the system is simplified by means of the following change of variables:

$$\theta = \frac{\bar{c}_p}{q_r}\left(T - T_s + \frac{q_l}{\bar{c}_p}\right) \quad (9)$$

$$X = \frac{\bar{c}_p}{4\pi\bar{\lambda}}\frac{m}{r}. \quad (10)$$

From which:

$$\frac{d\epsilon_i}{dX} = -\frac{\bar{c}_p}{\bar{\lambda}}\frac{X_s^2\,r_s^2}{X^4}\,w_i \quad (11)$$

$$\frac{d\theta}{dX} = -(\theta - \epsilon_3) \quad (12)$$

$$\sum_j \frac{Y_j}{M_j}\left[\left(\frac{\epsilon_j}{Y_j} - \frac{\epsilon_i}{Y_i}\right)\mathfrak{L}_{ij} + \frac{1}{Y_i}\frac{dY_i}{dX} - \frac{1}{Y_j}\frac{dY_j}{dX}\right] = 0 \quad (13)$$

where X_s, given by:

$$X_s = \frac{\bar{c}_p}{4\pi\bar{\lambda}}\frac{m}{r_s}, \quad (14)$$

is the new eigenvalue of the system. The boundary conditions are now as follows:

$$X = X_s\begin{cases} \theta = \theta_s \\ \epsilon_{1s} = 1 \\ \epsilon_{is} = 0 \quad (i \neq 1) \end{cases} \qquad X = 0\begin{cases} \theta = \theta_\infty \\ Y_{1\infty} = \epsilon_{1\infty} = 0. \\ Y_i = Y_{i\infty} \end{cases} \quad (15)$$

The solution of the problem lies on the integration of the nonlinear system of differential Equations (11), (12) and (13) with boundary conditions (15). In addition, an expression of w_i as a function of the mass fractions and temperatures should be known.

An analytical method will be developed to solve the system, which will be applicable, indistinctly, to both monopropellant and bipropellant droplets.

The law of variation of the functions

$$\epsilon_i(X) \quad \text{and} \quad \frac{d\epsilon_i}{dX}(X),$$

which was found by means of numerical integration of the equations for several typical cases,[8, 13, 15] suggested the adoption of an approximate analytical integration method. This method is based upon considering a reaction zone of finite thickness and on approaching the law of variation of ϵ_i within such zone by means of two parabolic curves tangent to each other at point $(\epsilon_{i\infty} + \epsilon_{is})/2$ and tangent to the lines $\epsilon_i = \epsilon_{i\infty}$ and $\epsilon_i = \epsilon_{is}$ at the boundaries of the reaction zone.

The reaction zone is determined by the values X_I and X_{II} of its hot and cold boundaries respectively, or else, by means of its central point X^* and thickness $\chi = X_{II} - X_I$. The maximum value of $d\epsilon_i/dX$, which will be called $\epsilon_i'^*$, should also be fixed.

The values of χ, $\epsilon_i'^*$ and X^* are obtained from the system of equations:

$$\left(\frac{d\epsilon_i}{dX}\right)_{X=X^*} = -\frac{\bar{c}_p}{\bar{\lambda}} \frac{X_s^2 \gamma_s^2}{X^{*4}} w_i^* = \epsilon_i'^* \tag{16}$$

$$\chi\epsilon_i'^* = 2\int_0^{X_s} \frac{d\epsilon_i}{dX}\, dX = 2(\epsilon_{is} - \epsilon_{i\infty}) \tag{17}$$

$$\left(\frac{d^2\epsilon_i}{dX^2}\right)_{X=X^*} = 0 \rightarrow X^* w_i'^* - 4w_i^* = 0 \tag{18}$$

In this system w_i^* is the value of $w_i(Y_i, \theta, X)$ for $X = X^*$, in which Y_i and θ are obtained by integrating differential Equations (12) and (13). This integration is performed by introducing into these equations the following expressions for ϵ_i :

$$\left(0 \leqslant X \leqslant X^* - \frac{\chi}{2}\right); \qquad \epsilon_i = \epsilon_{i\infty} \tag{19}$$

$$\left(X^* - \frac{\chi}{2} \leqslant X \leqslant X^*\right); \qquad \epsilon_i = \epsilon_{i\infty} - \frac{2(\epsilon_{i\infty} - \epsilon_{is})}{\chi^2}\left[X - \left(X^* - \frac{\chi}{2}\right)\right]^2 \tag{20}$$

$$\left(X^* \leqslant X \leqslant X^* + \frac{\chi}{2}\right); \qquad \epsilon_i = \epsilon_{is} + \frac{2(\epsilon_{i\infty} - \epsilon_{is})}{\chi^2}\left[X^* + \frac{\chi}{2} - X\right]^2 \tag{21}$$

$$\left(X^* + \frac{\chi}{2} \leqslant X \leqslant X_s\right); \qquad \epsilon_i = \epsilon_{is}. \tag{22}$$

The integration of Equation (12) is straightforward and expressions for θ are then readily derived. The eigenvalue X_s is obtained by integrating Equation (12) between θ_s and θ_∞.

The integration of expression (13) is more involved, because the equations are not linear. However, when the molecular weights of the species as well as the Lewis-Semenov numbers are equal, equation (13) reduces to:

$$\frac{dY_i}{dX} = -\mathfrak{L}(Y_i - \epsilon_i) \tag{23}$$

and the integration can readily be performed.

An approximate method has been developed[15] to integrate Equations (13) for the general case. This method is based on the series expansion of the expressions for Y_i, assuming that χ is small, which is the case that normally occurs in practice.

Several solutions[8, 13, 15] for typical cases of systems[11–13] given by the approximate analytical method have been compared to those obtained by the numerical integration of the equations. Comparisons were performed for a wide range of variation of the characteristic parameters of the process and for different reaction rates.

These comparisons showed that the approximation furnished by the analytical method was excellent in all practical cases.

Applications and Discussion of Results

MONOPROPELLANTS

The case corresponding to a first-order reaction of the form:

$$A_1 \rightarrow A_3; \qquad M_1 = M_3; \tag{24}$$

will be considered.

Therefore:

$$\epsilon_{1s} = 1; \quad \epsilon_{3s} = 0; \quad \epsilon_{1\infty} = 0; \quad \epsilon_{3\infty} = 1; \quad Y_{1\infty} = 0; \quad Y_{3\infty} = 1$$

The chemical kinetics of the process will be approximated by means of the over-all reaction rate:

$$w_3 = -w_1 = B\rho(1 - Y_3)e^{-E/RT} = \frac{\bar{\lambda}}{\bar{c}_p} A_M \frac{e^{-\theta_a/(\theta-\theta_0)}}{\theta - \theta_0}(1 - Y_3) \tag{25}$$

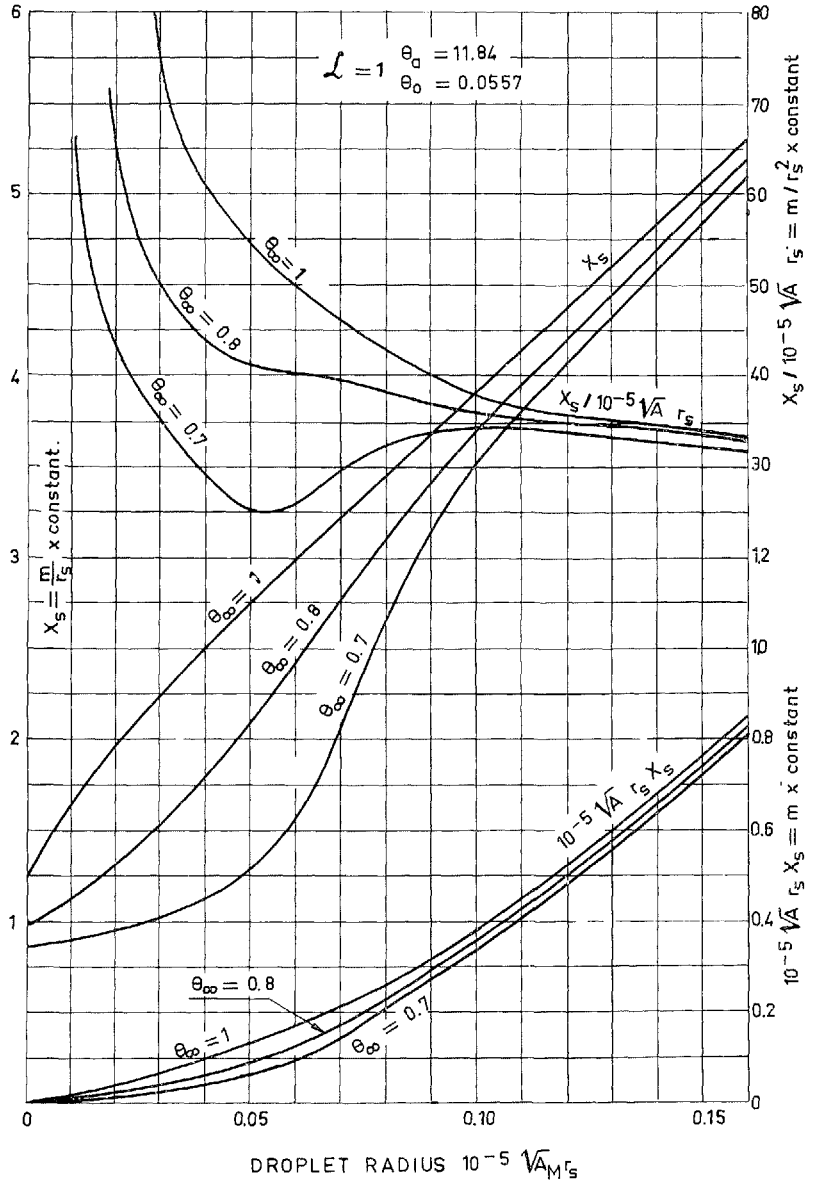

FIG. 1. Combustion of monopropellant droplets within an inert atmosphere. Burning rates, evaporation constants $\left(k \sim \frac{m}{r_s}\right)$ and burning rates per unit surface.

where:

$$A_M = \frac{B\rho_s T_s \bar{c}_p^2}{q_r \bar{\lambda}} \tag{26}$$

$$\theta_a = \frac{\bar{c}_p E}{R q_r} \tag{27}$$

$$\theta_0 = \frac{q_l - \bar{c}_p T_s}{q_r}. \tag{28}$$

Some results are shown in Figures 1, 2 and 3. In Figure 1, burning rates $m \sim r_s X_s$, evaporation constants $k \sim m/r_s \sim X_s$ and burning rates per unit surface $m/r_s^2 \sim X_s/r_s$ are plotted in function of the dimensionless droplet radius for several values of the temperature at infinity. It may be observed that m/r_s is not constant, but increases indefinitely as the radius of the droplets augments. This means that the linear

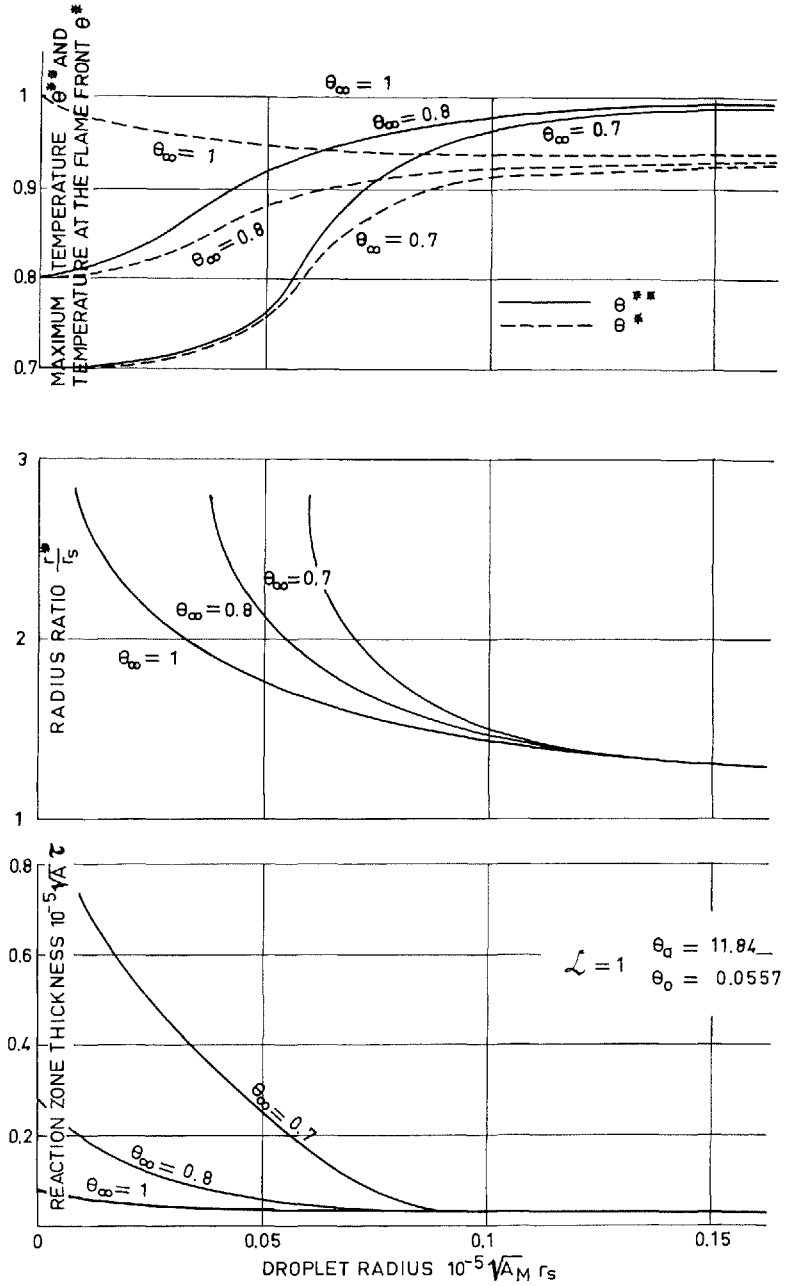

FIG. 2. Combustion of monopropellant droplets within an inert atmosphere. Temperatures, flame: droplet radius ratio and reaction zone thickness.

law of variation of the square of the droplet radius as a function of the time does not always hold for monopropellants.

For large values of r_s, the burning rate per unit surface tends toward a constant value, and when r_s tends toward zero the limiting value of X_s is given by:

$$(X_s)_{r_s \to 0} = \log \frac{\theta_\infty}{\theta_s} \tag{29}$$

which corresponds to the case of evaporation of droplets in the absence of combustion.

In Figure 2, temperatures, flame:droplet radius ratio and flame thickness $\tau = r_I - r_{II}$ are

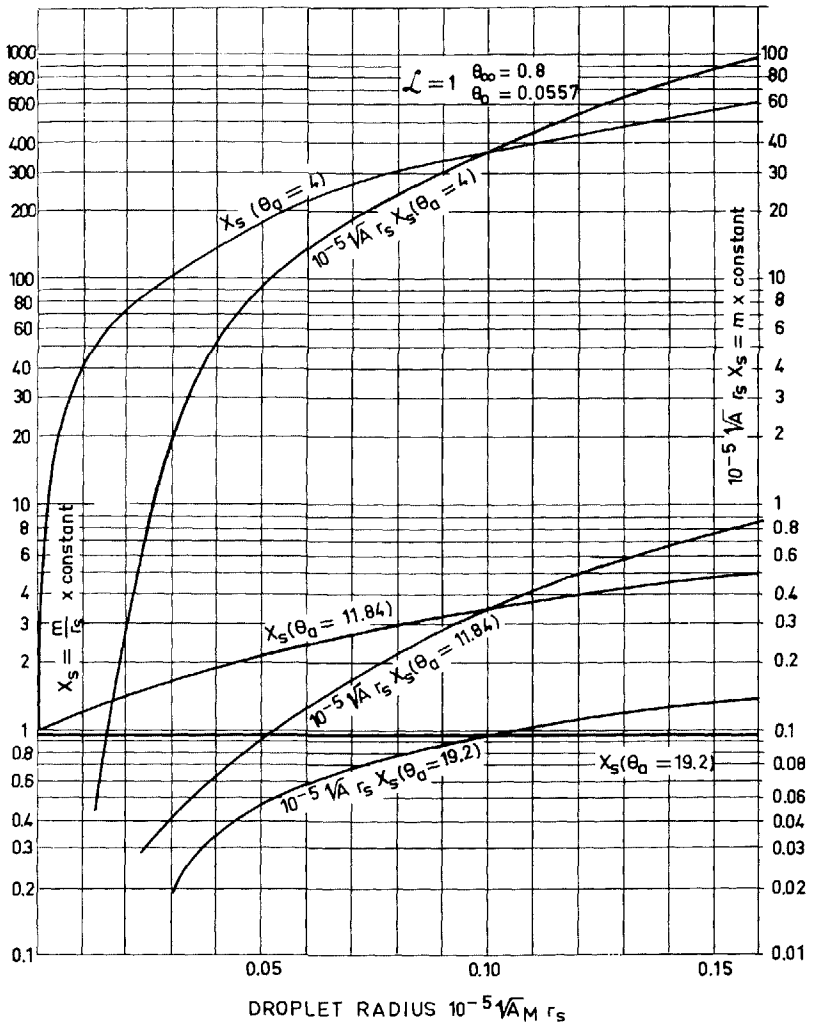

FIG. 3. Combustion of monopropellant droplets within an inert atmosphere. Influence of parameter θ_a, dimensionless ratio of the activation energy to the heat of reaction.

represented in function of the droplet radius. For large droplets, the maximum temperature θ^{**} is close to the equilibrium temperature for adiabatic combustion and the flame:droplet radius ratio tends toward unity. When the droplet radius tends toward zero θ^* and θ^{**} tend toward the temperature of the surrounding atmosphere, and the flame:droplet radius ratio tends toward infinity, which also correspond to the case of evaporation without combustion.

Figure 3 shows the fundamental influence of parameter θ_a (dimensionless ratio of the activation energy to the heat of reaction). From this figure and from the work cited in reference 13 it may be seen that, for an average sized droplet, when θ_a is small combustion is rapid, the flame is close to the droplet surface, and the maximum temperature is almost equal to the equilibrium temperature for adiabatic combustion. On the contrary, when θ_a is large, combustion is slow, the flame is far from the droplet surface and the maximum temperature is close to the temperature of the surrounding atmosphere. However, when the droplet radius tends toward zero, the limiting value of the burning rate does not depend on θ_a, because it tends toward the limiting value given by Equation (29).

In Figure 4 some results obtained for the combustion of hydrazine droplets in an inert atmosphere are given. They were derived for a

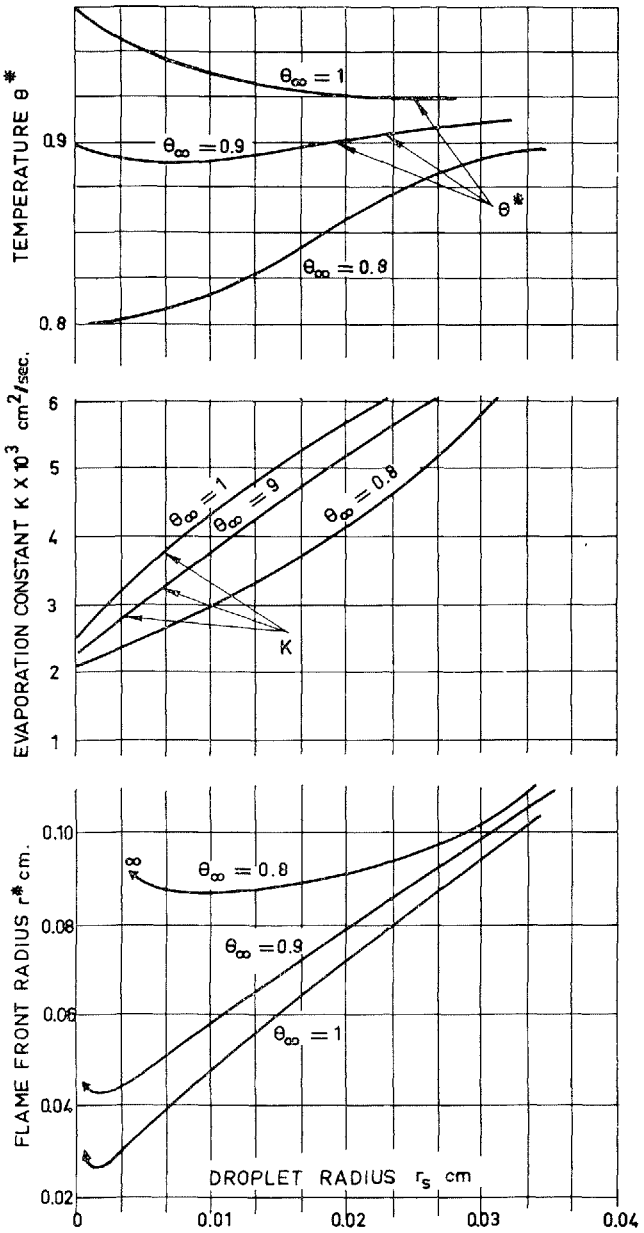

FIG. 4. Combustion of hydrazine droplets within an inert atmosphere. Theoretical results

reaction rate obtained by applying the steady-state assumption for the radicals to the decomposition reaction model for hydrazine proposed by Adams and Stock.

BIPROPELLANTS

The following over-all reaction will be considered:

$$A_1 + A_2 \rightarrow 2A_3\,, \qquad (30)$$

and the chemical kinetics of the process will be approximated by means of the over-all reaction rate:

$$w_3 = \frac{2M_3^2}{M_1 M_2}\frac{\bar{\lambda}}{\bar{c}_p} A_B \frac{e^{-\theta_a/(\theta-\theta_0)}}{(\theta-\theta_0)^2} Y_1 Y_2 \qquad (31)$$

in which θ_a and θ_0 are given by Equations (27) and (28) and A_B is defined by

$$A_B = \frac{\bar{c}_p^3 (\rho_s T_s)^2 B}{\bar{\lambda} q_r M_3}\,. \qquad (32)$$

Results obtained in function of the droplet radius showed that all solutions lie between two limiting cases:

When $r_s \to 0$ results correspond to the case of evaporation of droplets in the absence of combustion, as for the combustion of monopropellant droplets. Therefore, X_s is given by Equation (29), θ^* tends toward θ_∞ and r^*/r_s tends toward infinity.

On the other hand, when r_s tends toward infinity, the limiting values are equal to those obtained by assuming an infinite reaction rate. The maximum temperature θ^{**}, the eigenvalue X_s, the radius ratio r^*/r_s, *etc.*, tend toward asymptotic values which can also be directly derived by taking an infinite reaction rate in systems (11), (12), (13), which implies that Equation (11) be disregarded and that the existence of a zero thickness flame may be assumed.[15] For example, the asymptotic value for X_s is given by:

$$(X_s)_{r_s\to\infty} = \log\left[\frac{\epsilon_{3\infty}}{\theta_s}\left(\frac{\epsilon_{3\infty} - Y_{3\infty}}{\epsilon_{3\infty} - 1}\right)^{1/\mathcal{L}_{23}} - \frac{1}{\theta_s}(\epsilon_{3\infty} - \theta_\infty)\right]. \tag{33}$$

Results will be shown for two representative cases:

1. Equal molecular weights and Lewis-Semenov numbers equal to unity

$$(M_1 = M_2 = M_3 = 20;$$
$$\mathcal{L}_{12} = \mathcal{L}_{23} = \mathcal{L}_{13} = 1).$$

Therefore:

$$\epsilon_{1\infty} = 0; \quad \epsilon_{2\infty} = -1; \quad \epsilon_{3\infty} = 2;$$
$$\epsilon_{1s} = 1; \quad \epsilon_{2s} = \epsilon_{3s} = 0.$$

2. Molecular weight M_2 of the gaseous reactant surrounding the droplet much smaller than molecular weight M_1 of the reactant from the droplet.

The following values have been taken:

$$M_1 = 38; \quad M_2 = 2; \quad M_3 = 20;$$
$$\mathcal{L}_{12} = \mathcal{L}_{23} = 0.45; \quad \mathcal{L}_{13} = 1.18$$
$$\epsilon_{1\infty} = 0; \quad \epsilon_{2\infty} = -0.052;$$
$$\epsilon_{3\infty} = 1.052; \quad \epsilon_{1s} = 1; \quad \epsilon_{2s} = \epsilon_{3s} = 0.$$

In order to compare results, the mean molecular weights of the mixtures have been taken to be equal for both cases, and the Lewis-Semenov numbers $\mathcal{L}_{ij}$ have been assumed to be proportional to

$$\sqrt{M_i M_j/(M_i + M_j)}.$$

Figures 5, 6 and 7 show results for the first case. Because parameter A_B is usually very large ($>10^{10}$ cm^{-2}) the results are generally close to their asymptotic values, provided that the droplets are not too small. This explains why the assumption of an infinite reaction rate leads to rather good results in many cases. However, if the value of parameter θ_a is large (weak reactions or high activation energies), the results may be very far from their limiting values, even for large droplets, as shown in Figure 7.

Figure 8 shows results for the second case, as well as a comparison of the values of X_s for both cases. It may be observed that for this case the results tend much more slowly toward their asymptotic values, which means that the assumption of an infinite reaction rate may introduce important errors when M_2 is much smaller than M_1.

It is doubtful that solutions close to the case of pure evaporations ($r_s \to 0$) actually represent real combustion processes, because the temperature profiles are very flat and the reaction zones are very wide.[15] Therefore, the results suggest the possibility that there may be a minimum size for the droplets below which combustion is not possible. If this is so, the minimum radius should be a very sensitive function of parameter θ_a.

Influence of Pressure

Influence of pressure is practically disregarded when assuming an infinite value of the reaction rate. On the contrary, results obtained considering chemical kinetics show that the influence of pressure may be very important for certain conditions.

Parameters A_M and A_B are proportional to p^n, where n is the order of the over-all chemical reaction. Therefore, all results have been obtained as a function of the dimensionless product $p^{n/2} \times r_s$ ($n = 1$ for monopropellants and $n = 2$ for bipropellants). It follows that for a droplet of given size results depend upon the pressure as they depended upon the droplet radius at constant pressure.

When pressure approaches infinity results tend toward an asymptotic value, which is directly obtained by taking an infinite reaction rate. If parameter θ_a is small, results are close

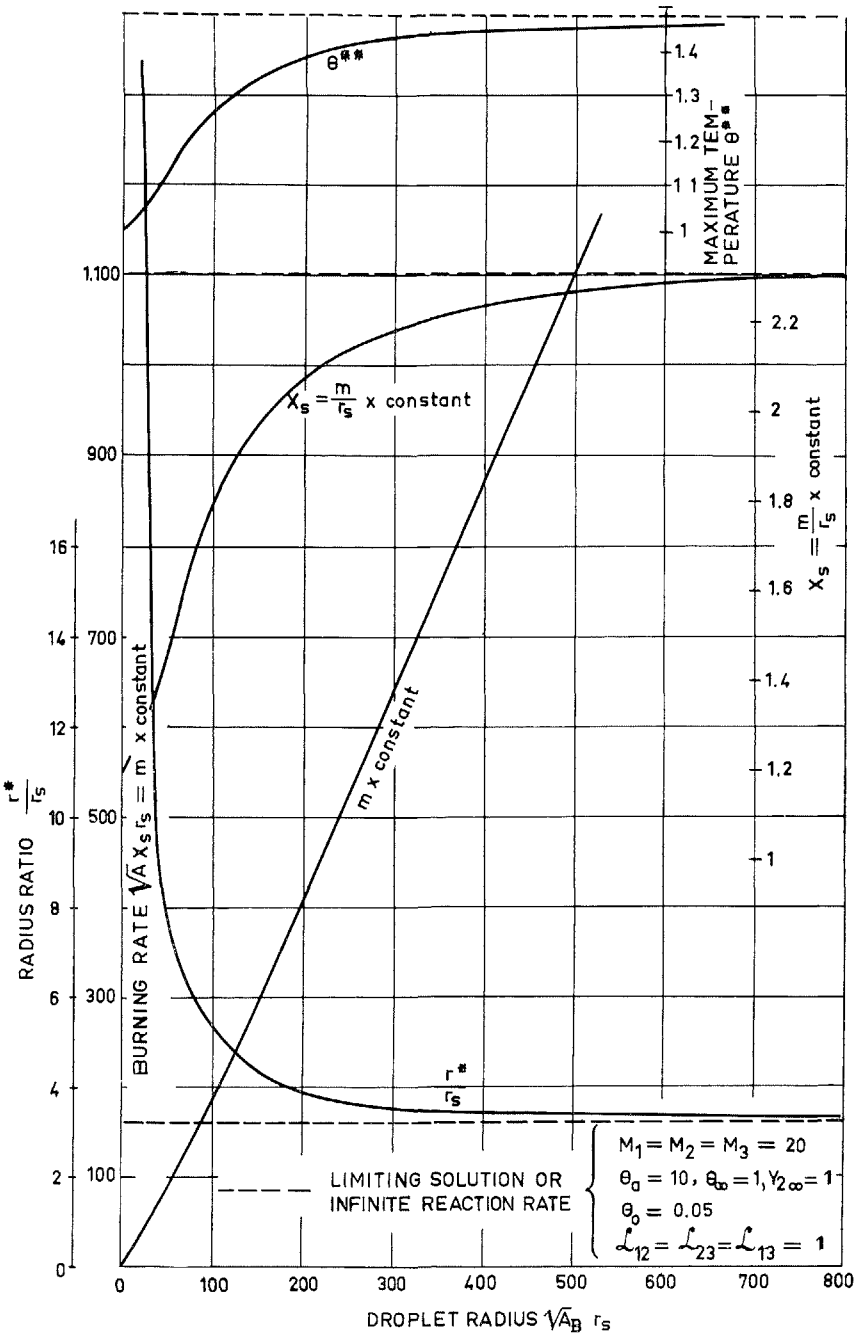

FIG. 5. Combustion of fuel or oxidizer droplets within the vapors of an oxidizer or fuel. Results for finite reaction rates and limiting solutions for an infinite reaction rate.

to their asymptotic values even for small values of product $p^{n/2} \times r_s$. Therefore, for such conditions the influence of pressure might be unnoticeable, unless very small droplets were studied (Fig. 9).

On the other hand, when pressure tends toward zero, results tend to correspond to those obtained in the evaporation of droplets in absence of combustion. Therefore, for small values, pressure may influence considerably the combus-

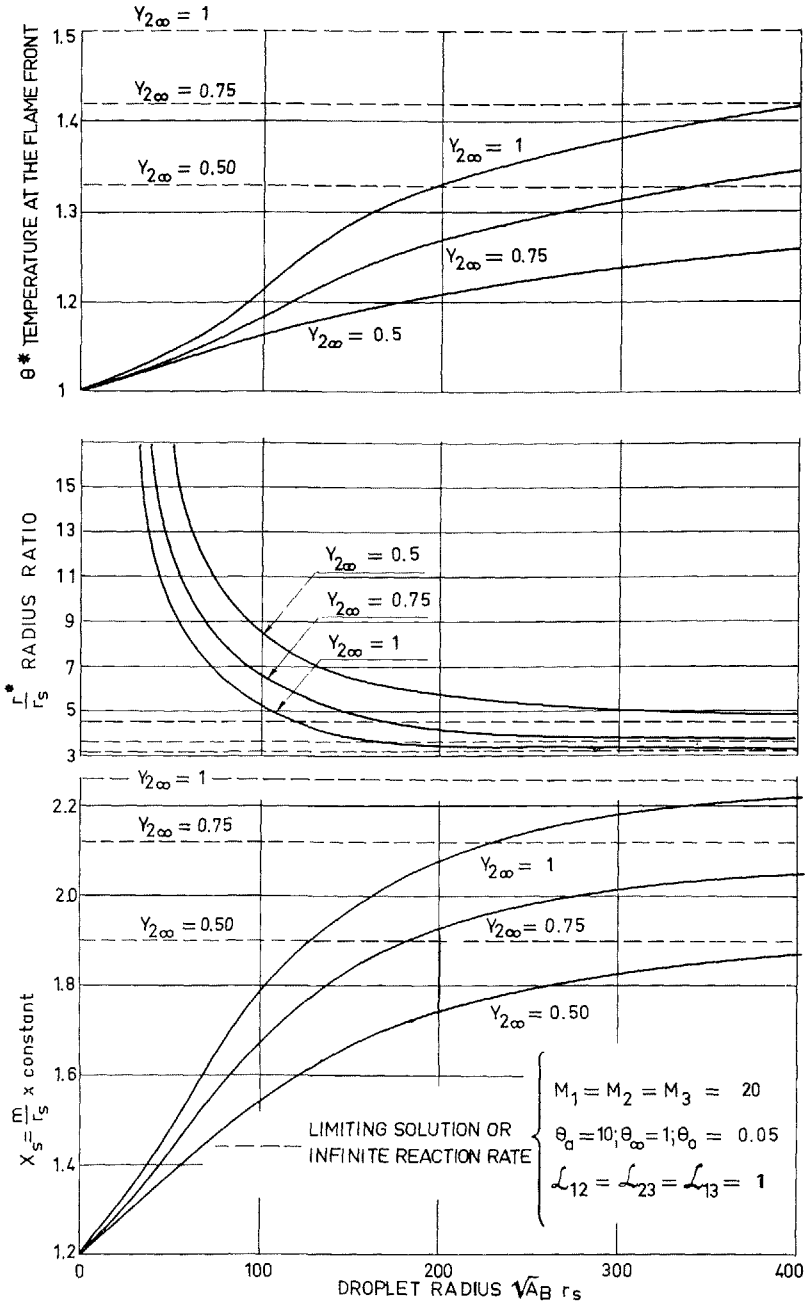

FIG. 6. Combustion of fuel or oxidizer droplets. Influence of $Y_{2\infty}$ mass fraction of the oxidizer or fuel at great distance from the droplet.

tion process, especially when the gaseous component surrounding the droplet has a low molecular weight.

For a droplet of constant size, as pressure decreases burning rate, evaporation constant and maximum temperature also decrease, while ratio r^*/r_s and flame thickness increase until a minimum value of the pressure is reached under which combustion seems no longer possible.

Experimental Results

MONOPROPELLANTS

A research facility was prepared to study combustion of monopropellant droplets with the

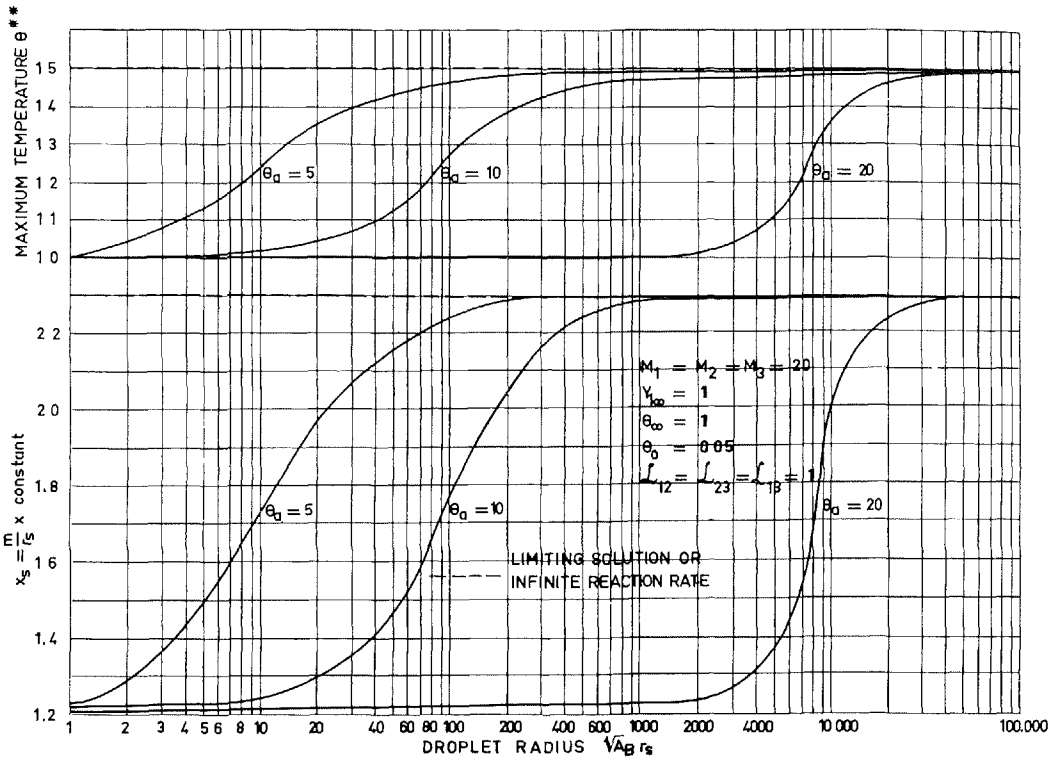

FIG. 7. Combustion of fuel or oxidizer droplets within the vapors of an oxidizer or fuel. Influence of parameter θ_a , dimensionless ratio of the activation energy to the heat of reaction.

quartz fiber technique. Droplets suspended from a thin quartz fiber were introduced into an electric furnace, where a mixture of oxygen and nitrogen could be maintained at constant temperature (Fig. 10).

Hydrazine, ethyl nitrate and a mixture of nitric acid and amyl acetate were tested. In all cases it was found that a minimum fraction of oxygen was always required to obtain combustion.

Burning rates and evaporation constants were measured at different temperatures and for several compositions of the gaseous mixture. Results for hydrazine are shown in Figure 11. It may be observed that for every composition of the mixture there existed an ignition temperature, which decreased appreciably as the oxygen concentration was raised.

Below the ignition temperature, the values of the evaporation constant coincide, for all mixtures, with those obtained in a pure nitrogen atmosphere. On the other hand, these values were close to those obtained by calculating the evaporation of hydrazine droplets in the absence of combustion.

An accurate comparison between theoretical and experimental results cannot be made, because combustion of monopropellant droplets in an absolutely inert atmosphere was not achieved. Furthermore, the form of the function $k = f(T)$ could not be determined accurately because of the scattering of the results. It may simply be mentioned that experimental values of the burning rates, especially those obtained when the concentration of oxygen was small, are of the same order of magnitude as the ones calculated theoretically for the combustion of hydrazine droplets in an inert atmosphere.

It may also be pointed out that for mixtures rich in oxygen the flame had an elongated shape, but when the concentration of oxygen was small the shape of the flame was almost spherical (Fig. 12).

Similar results were obtained when using the other types of monopropellants already mentioned.

BIPROPELLANTS

In order to verify several theoretical conclusions, a research facility was prepared to

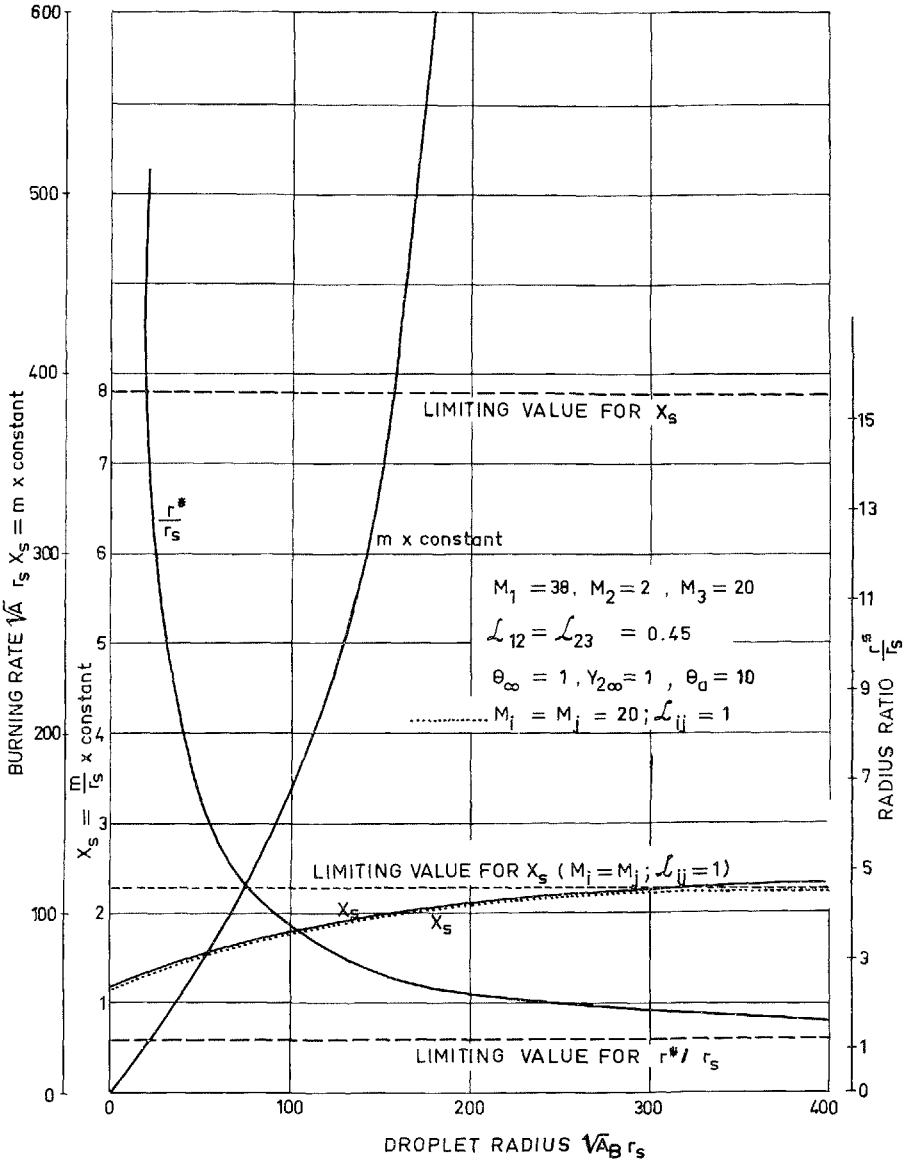

FIG. 8. Combustion of fuel or oxidizer droplets within the vapors of an oxidizer or fuel. Results obtained when the gaseous component surrounding the droplet has a low molecular weight.

observe combustion of droplets for different propellant combinations at variable pressure (from $\frac{1}{10}$ up to 10 atmos). The facility was also suitable for studying combustion of oxidizer droplets in a hydrogen atmosphere. Hydrogen was selected because of its low molecular weight, which prevents natural convection effects and makes the influence of chemical kinetics more noticeable.

The research facility is shown in Figure 13. Droplets suspended from a quartz fiber are introduced into a glass tube filled with CO_2, closing simultaneously the tube inlet. The tube is then moved downward by means of an electromagnetic actuator, and the droplet is ignited by two electrodes which are placed in position by the motion of the tube.

Combustion of bromine droplets was observed first, for the purpose of comparing theoretical and experimental results, because chemical

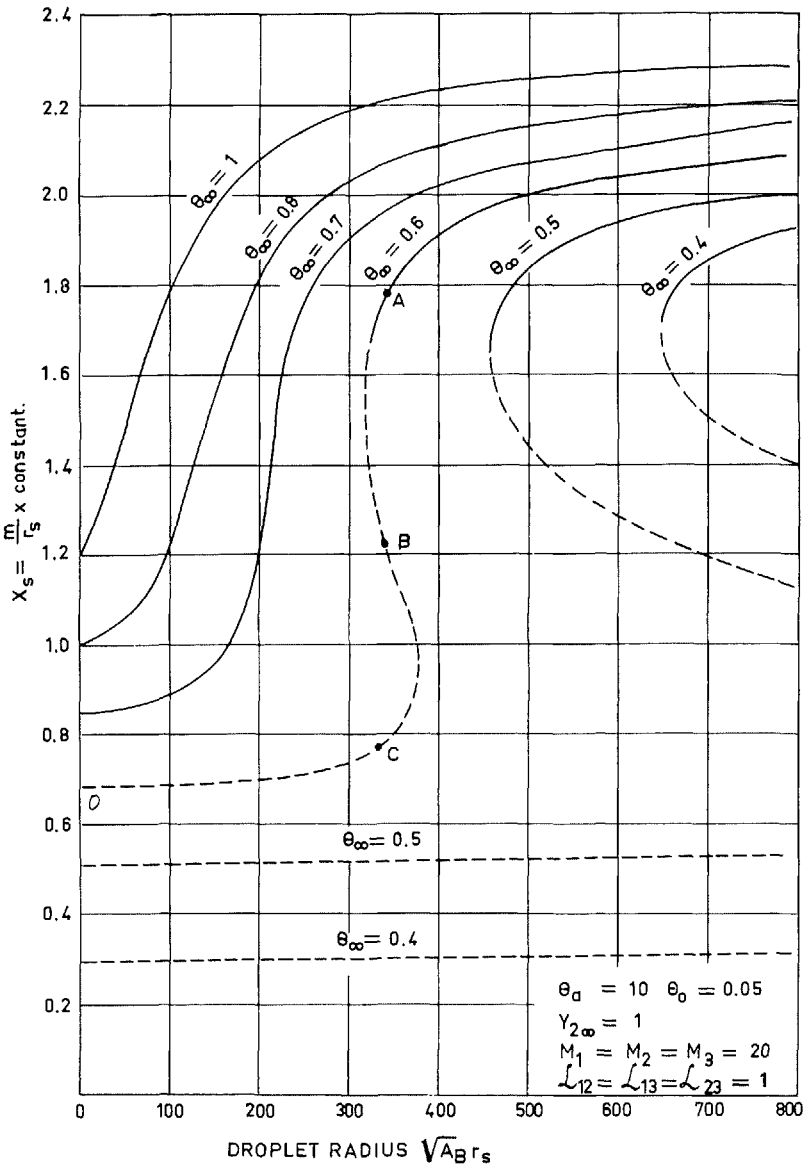

FIG. 9. Combustion of droplets. Eigenvalue X_s in function of the droplet radius. When θ_∞ is small there exist three possible values of X_s, for each value of r_s, which correspond to three mathematical solutions of the process.

kinetics of the hydrogen-bromine reaction is known.

It was verified that for droplets with an initial radius r_{si} of about 0.5 mm, combustion did not occur up to pressures of the order of 4 atmos. Slopes of curves $r_s^2 = f(t)$ were measured by means of a kinematographic camera, but the flame radius could not be measured because the flame was hardly visible.

By applying the steady-state assumption for the radicals to the hydrogen-bromine reaction model proposed by Campbell and Hirschfelder,[b] an over-all reaction rate of $\frac{3}{2}$ order was obtained, which was utilized to study the combustion of bromine droplets in hydrogen by applying the analytical method previously described. In

[b] C.F. 2108. University of Wisconsin, 1953.

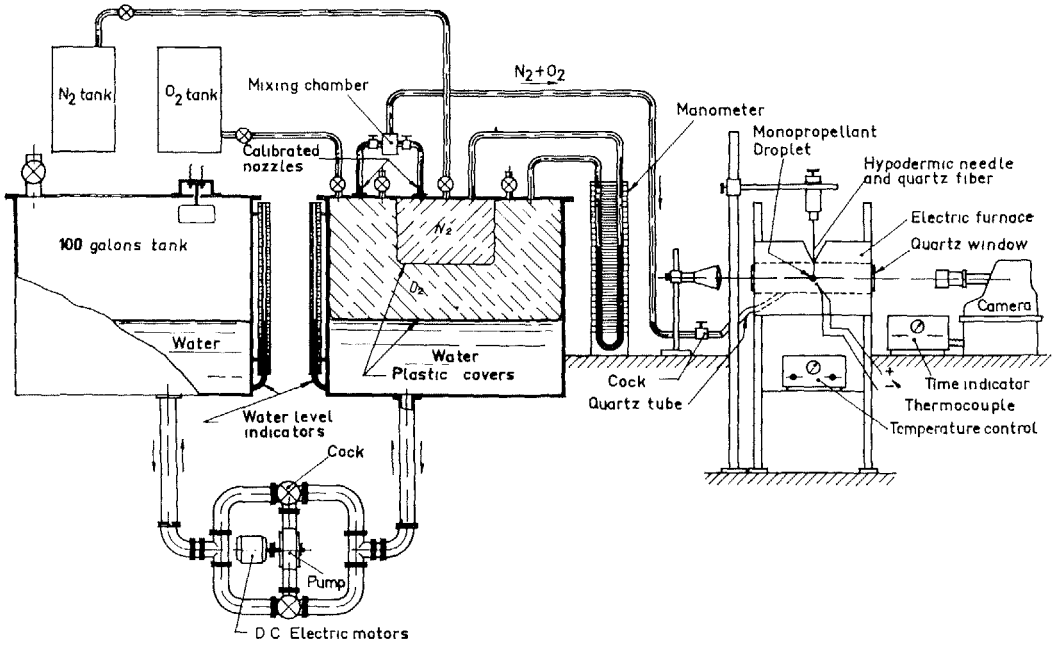

FIG. 10. Schematic diagram of apparatus used to observe combustion of monopropellant droplets within a mixture of oxygen and nitrogen.

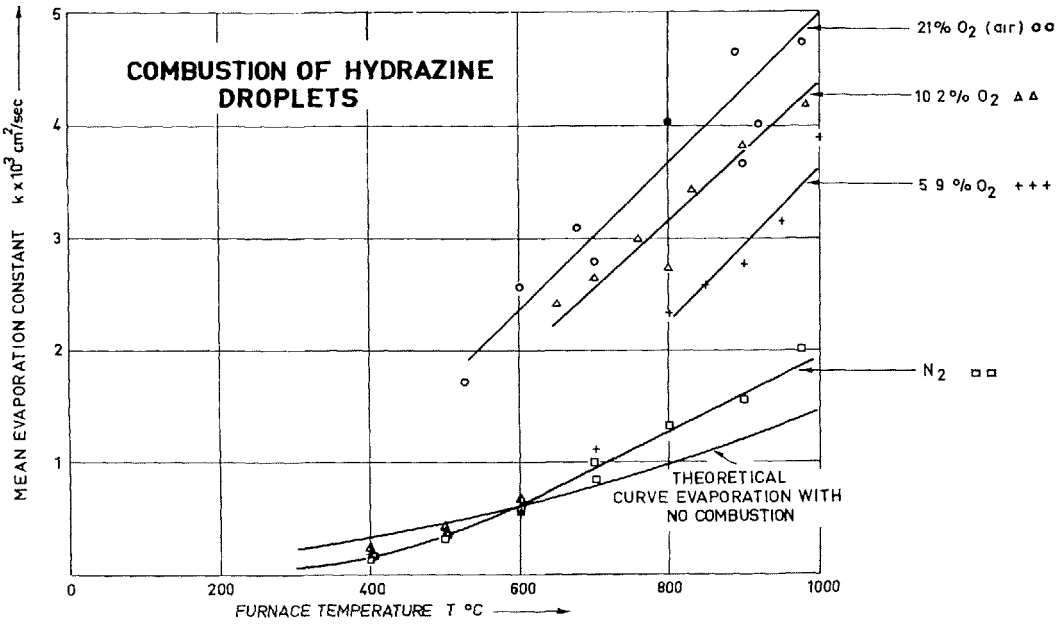

FIG. 11. Combustion of hydrazine droplets. Experimental results

Figure 14 the theoretical values obtained for the evaporation constants, k, as a function of pressure are shown, as well as some experimental results. The theoretical curve $k = f(p)$ shows that for droplets of initial radius of 0.5 mm combustion is not possible for pressures under 5.5 atmos, which agrees rather well with the experimental results.

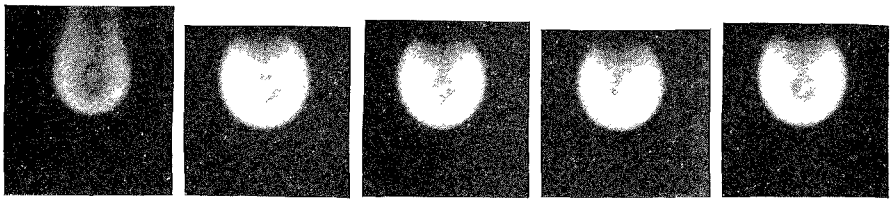

$t \approx 0$ $t = \frac{1}{16}$ sec $t = \frac{2}{16}$ sec $t = \frac{3}{16}$ sec $t = \frac{4}{16}$ sec

FIG. 12. Hydrazine droplet burning in a mixture of 90% N_2 and 10% O_2 Furnace temperature T_∞ = 650°C.

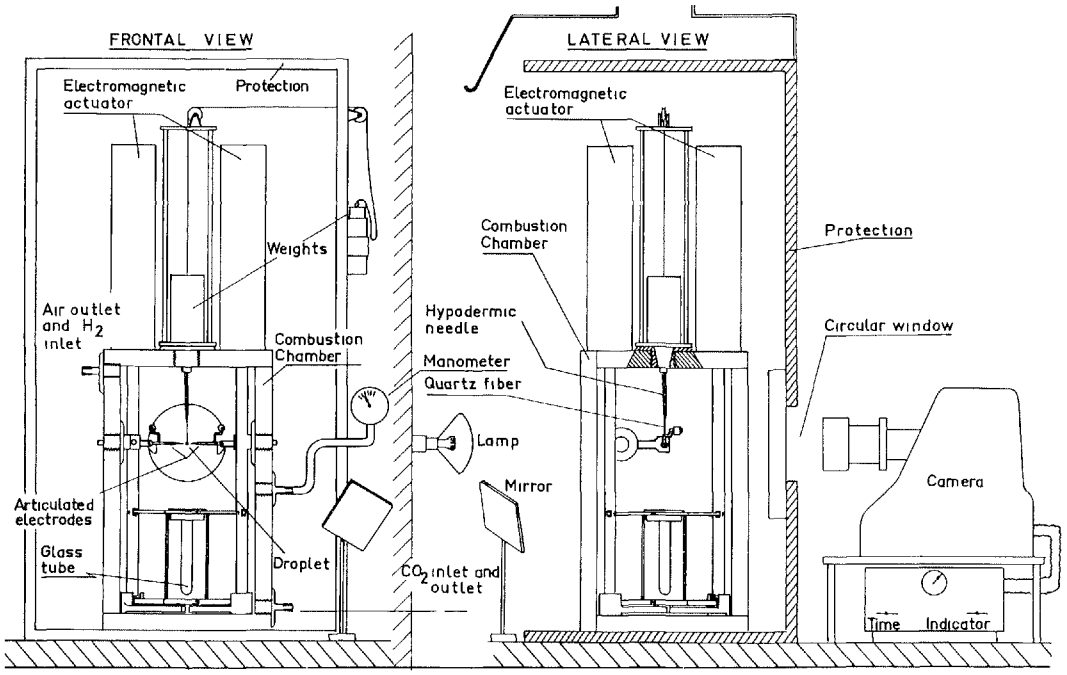

FIG. 13. Schematic diagram of apparatus used to observe combustion of oxidizer droplets within a hydrogen atmosphere.

Combustion of bromine droplets was very fast (a droplet of 1 mm in diameter burns in $\frac{1}{10}$ of a second), which produced an important scattering of results. This prevented the formulation of any law of variation of the evaporation constants as a function of pressure However, the experimental and theoretical values were of the same order of magnitude.

Combustion of nitric acid droplets in hydrogen was also observed. No precise data were available on the combustion mechanism of this reaction. It was not possible, therefore, to compare theoretical and experimental results.

Photographs of a burning droplet are shown in Figure 15, in which it may be observed that the flame is spherical. This allows a precise measurement of the flame diameter, assumed to be equal to the illuminated zone of the photographs. Some experimental results are shown in Figure 16. Curves $r_s^2 = f(t)$ were approximated by means of straight lines, and the resulting average values for k are given in the figure

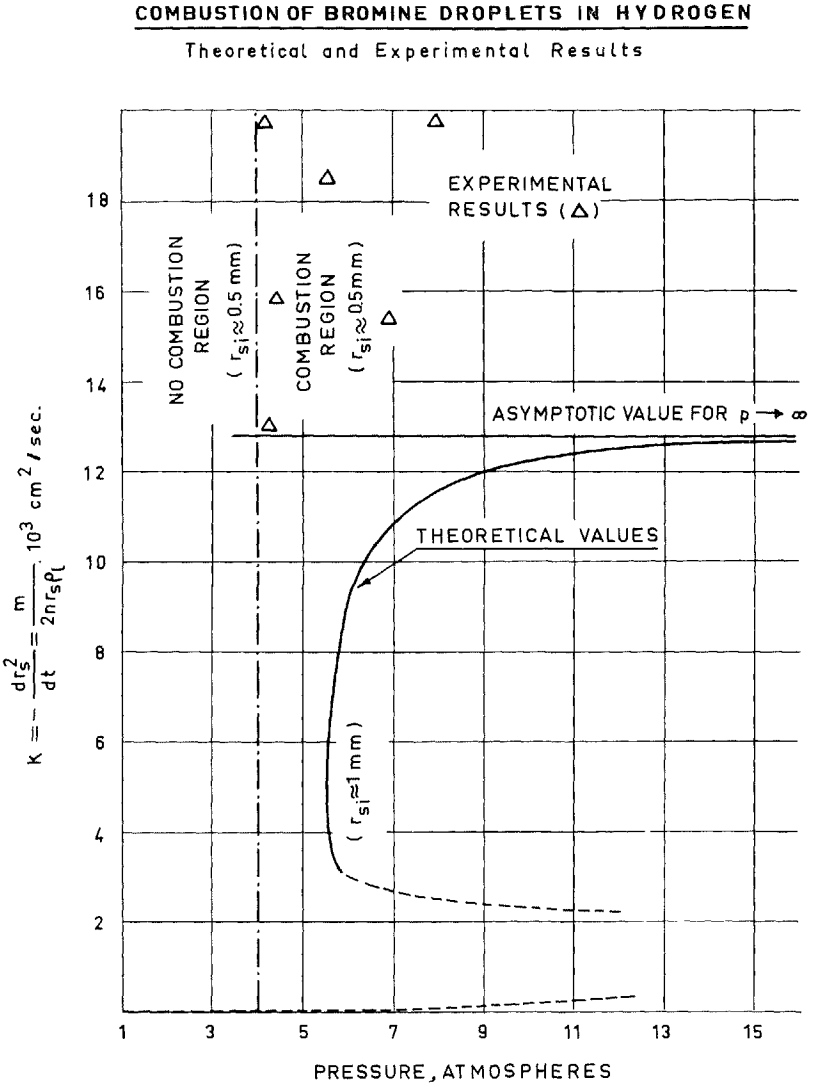

FIG. 14. Combustion of bromine droplets in hydrogen. Theoretical and experimental results

Results for the flame:droplet radius ratio $r^*:r_s$ show that its value is not constant but increases as the droplet radius decreases in a manner similar to that predicted theoretically.

Combustion in air at low pressure of several types of fuel droplets were observed also. In Figure 17 photographs of *n*-heptane droplets burning in air at low pressure are shown. As the pressure is reduced, the flame becomes larger and darker and its shape is almost spherical, which means that the combustion temperature is lower according to the results calculated theoretically.

In Figures 18 and 19 results obtained for the evaporation constants and for the flame:droplet radius ratio are shown. The form of functions $k = f(p)$, $k = f(p^{0.6}\bar{r}_s)$,[c] $r^*:r_s = f(r_s)$ and $r^*:r_s = f(p^{0.6}r_s)$ are in excellent qualitative agreement with the general results obtained

[c] $\bar{r}_s$ represents an average value between the initial and final measured radius.

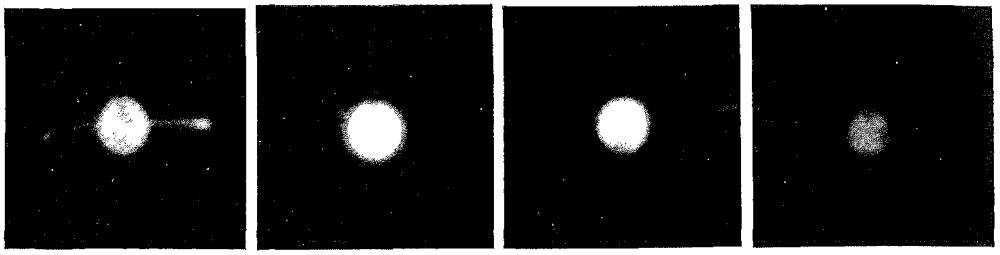

$t \approx 0$ $t = \frac{1}{12}$ sec $t = \frac{2}{12}$ sec $t = \frac{3}{12}$ sec

FIG. 15. Nitric acid droplet burning in hydrogen. Natural convection effects do not exist. Magnification ratio 5/1.

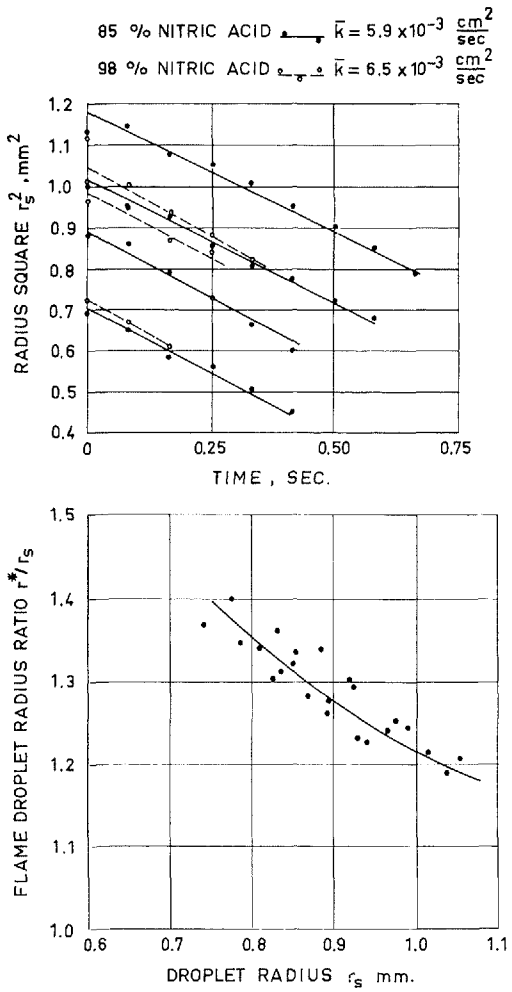

FIG. 16. Combustion of nitric acid droplets within hydrogen. Experimental results.

theoretically for the combustion of bipropellant droplets.

Finally, in Figure 20, minimum values of the droplet radius for combustion r_{s0} are shown as a function of the pressure for *n*-heptane and ethyl alcohol droplets. Such radius r_{s0} represents the minimum values for which ignition could not be achieved by means of electric sparks, and sometimes the extinction values of the radius after a short combustion of the type shown in Figure 17b.

The influence of the ignition mechanism on the process and the possible influence of the stability of the flame on the extinction process prevented the formulation of any precise law of variation of the extinction radius as a function of pressure. However approximated results may be obtained from this figure.

Nomenclature

A_M , A_B	constants of the reaction rate equations for monopropellants and bipropellants, respectively
B	frequency factor
c_p	specific heat at constant pressure
$\bar{c}_p$	average value of c_p for the mixture
D_{ij}	diffusion coefficient
E	activation energy
h_i	specific enthalpy
k	evaporation constant
m	burning rate
M_i	molecular weight
p	pressure
q_l	latent heat of evaporation
q_r	heat of reaction
r	radius
r_s	droplet radius

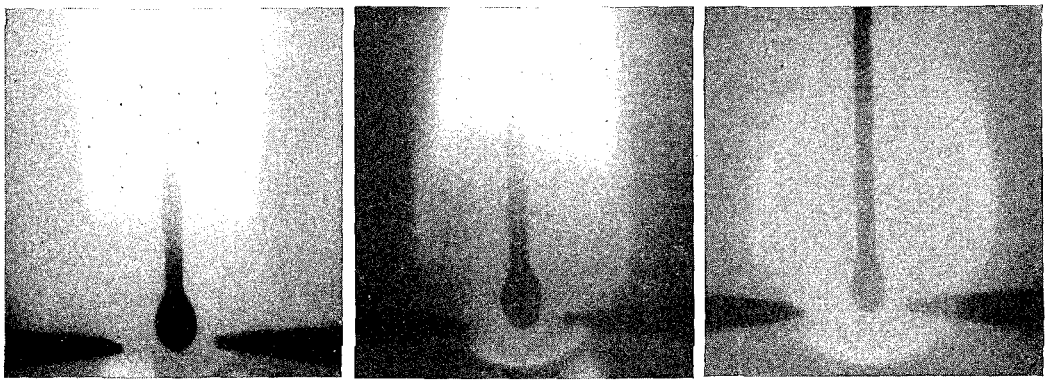

Left: $p = 1$ atmos *Center:* $p \approx \frac{2}{3}$ atmos *Right:* $p \approx \frac{1}{3}$ atmos

FIG. 17a. Combustion in air of n-heptane droplets of equal size at different pressures. Magnification ratio 4:5/1.

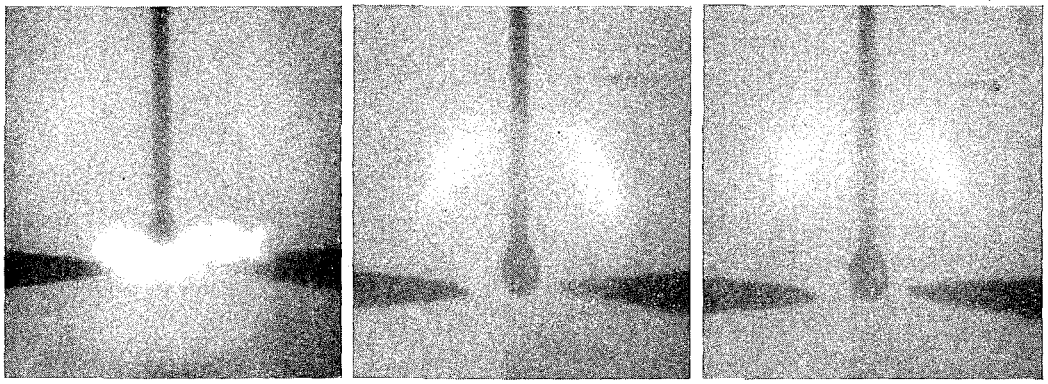

Left: $t \approx 0$ *Center:* $t = \frac{1}{4}$ sec *Right:* $t = \frac{1}{2}$ sec (Extinction of the flame)

FIG. 17b. Combustion in air of a n-heptane droplet at $\frac{1}{4}$ of atmosphere. Magnification ratio 4:5/1.

R	gas constant
t	time
T	absolute temperature
w_i	reaction rate
X	$= \bar{c}_p m/4\pi\bar{\lambda}r$, dimensionless coordinate
X_s	$= \bar{c}_p m/4\pi\bar{\lambda}r_s$, eigenvalue of the system, proportional to the evaporation constant
Y_i	mass fraction
ϵ_i	ratio of flux of mass of species i to total mass flow
λ	thermal conductivity
$\bar{\lambda}$	average value of λ for the mixture
$\mathfrak{L}_{ij}$	$= \bar{\lambda}/\rho D_{ij}\bar{c}_p$, Lewis-Semenov number
ν_i	stoichiometric coefficients of chemical reaction
ρ	gas density
θ	dimensionless temperature
θ_0	constant
χ	reaction zone thickness at the X coordinate system
τ	actual reaction zone thickness

SUBSCRIPTS

i, j	reactant species
1	gaseous reactant from the droplet (fuel, oxidizer or monopropellant vapors)
2	gaseous reactant surrounding the droplet (fuel or oxidizer)
3	reaction products
I, II	limiting points of the assumed finite reaction zone
s	on the droplet surface

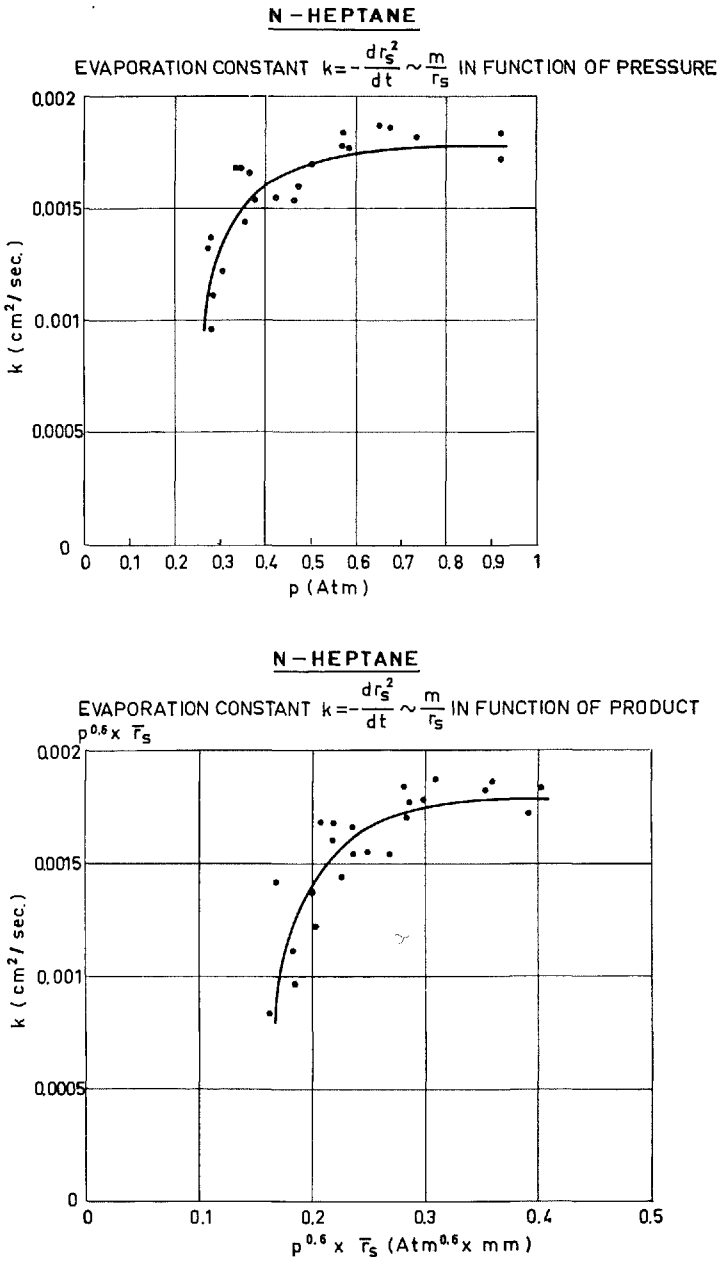

FIG. 18. Combustion of *n*-heptane droplets in air. Experimental values of the evaporation constants.

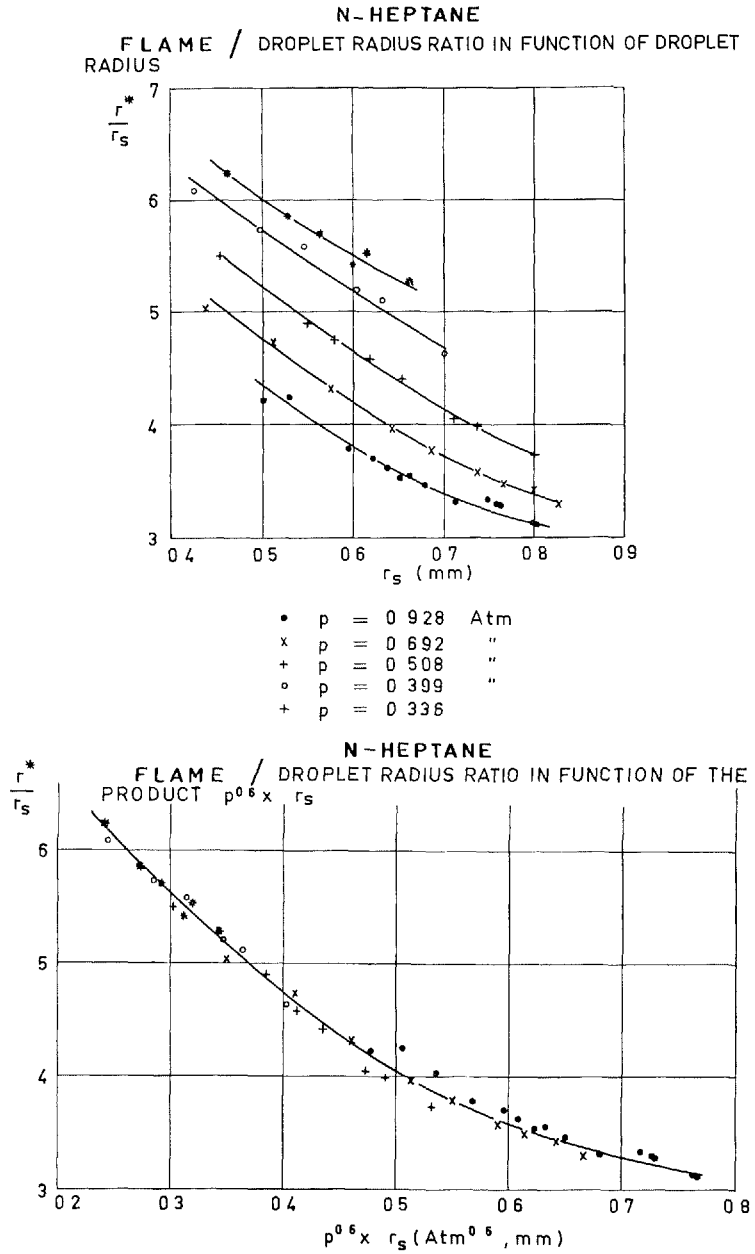

FIG. 19 Combustion of *n*-heptane droplets in air. Experimental values of the flame:droplet radius ratio.

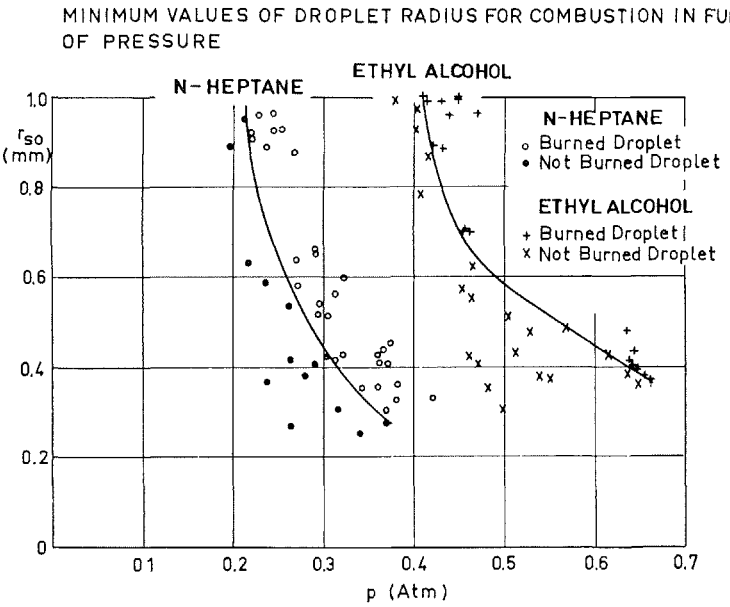

FIG. 20. Combustion of *n*-heptane and ethyl alcohol droplets in air. Experimental values of the minimum droplet radius for combustion.

SUPERSCRIPTS

*	center of the reaction zone (point at which $d\epsilon_i/dX$ is a maximum)
**	point of maximum value of the temperature
′	derivative with respect to X
0	standard state

REFERENCES

1. GODSAVE, G. A. E.: *Fourth Symposium (International) on Combustion*, The Williams & Wilkins Company, Baltimore, 1953.
2. GOLDSMITH, M., AND PENNER, S. S.: California Institute of Technology, 1953.
3. HALL, A. R., AND DIEDERICHSEN, J.: *Fourth Symposium (International) on Combustion*, The Williams & Wilkins Company, Baltimore, 1953.
4. WISE, H., LORELL, J., AND WOOD, B. J.: *Fifth Symposium (International) on Combustion*, Reinhold Publishing Corporation, New York, 1955.
5. LORELL, J., WISE, H., AND CARR, R. S.: Proceedings of the Gas Dynamics Symposium on Aerothermochemistry, 1956. Northwestern University, Evanston Ill.
6. BARRÈRE, M., AND MOUTET, H.: Étude experimentale de la Combustion de Gouttes de Monergol. La Recherche Aéronautique, No. 50, 1956.
7. AGOSTON, A. G., WISE, H., AND ROSSER, W. A.: *Sixth Symposium (International) on Combustion*, p. 708. Reinhold Publishing Corporation, New York, 1957.
8. SÁNCHEZ TARIFA, C., AND SALAS LARRAZÁBAL, J. M.: INTA, ARDC Contract No. AF 61(514)-997, Madrid, 1957.
9. BOLT, J. A., AND SAAD, M. A.: *Sixth Symposium (International) on Combustion*, p. 717. Reinhold Publishing Corporation, New York, 1957.
10. KUMAGAI, S., AND ISODA, H.: *Sixth Symposium (International) on Combustion*, p. 726. Reinhold Publishing Corporation, New York, 1957.
11. ISODA, H., AND KUMAGAI, S.: *Seventh Symposium (International) on Combustion*, Butterworth and Company, Ltd., London, 1958.
12. WILLIAMS, F.: California Institute of Technology, TR No. 21, 1958.
13. SÁNCHEZ TARIFA, C., AND PÉREZ DEL NOTARIO, P.: INTA AFOSR Doc. No. TN 58-1038, Madrid, 1958.
14. PÉREZ DEL NOTARIO, P., AND SÁNCHEZ TARIFA, C.: INTA ARDC Contract No. AF 61 (514)-997, Madrid, 1959.
15. SÁNCHEZ TARIFA, C., AND PÉREZ DEL NOTARIO, P.: INTA ARDC Contract No. AF 61 (052)-221, Madrid, 1960.